The on-ground calibrations of SuperAGILE: II Finite distance radioactive sources

I. Donnarumma[a], E. Costa[a], E. Del Monte[a], G. Di Persio[a], Y. Evangelista[a], M. Feroci[a], M. Frutti[a], I. Lapshov[a], F. Lazzarotto[a], A. Lo Bue[b], M. Mastropietro[a,c], E. Morelli[d], L. Pacciani[a], G. Porrovecchio[a], M. Rapisarda[b], P. Rossi[b], A. Rubini[a], G. Sabatino[a], P. Soffitta[a]

[a]INAF-IASF Roma, Via Fosso del Cavaliere 100, Rome, Italy
[b]ENEA, Fusione Tecnologie C.R., Frascati, Italy
[c]ISC CNR, Via Salaria km 29.300, I-00016 Monterotondo Scalo (RM), Italy
[d]INAF-IASF Bologna, Via P. Gobetti 101, I-40129 Bologna, Italy

ABSTRACT

The Flight model of SuperAGILE experiment was calibrated on-ground on August 2005 at IASF-Rome laboratories using standard radioactive X-rays sources. These omnidirectional sources were positioned at approximately 2 meters distance from the experiment. A method to correct for the beam divergence has been developed in order to use these measurements to derive information about the point spread function of the experiment for infinite distance sources. In this paper we describe the set-up of the measurements, the method to correct for the beam divergence and show preliminary results of the data analysis.

Keywords: coded mask, calibration, X-rays

1. INTRODUCTION

SuperAGILE is a one-dimension coded mask experiment. It is designed to operate in the nominal energy range 15-45 keV, providing one-dimensional images of the sky in two ortogonal directions in a wide field of view (~ 1.5 radians). The field of view of SuperAGILE is limited by a collimator, with aperture covered by 4 coded masks. The masks code is a Hadamard sequence of 787 elements generated with the method of quadratic residue, to which one element has been added to reach the complete symmetry and reversibility of the mask. Each nominal mask element is 242 μm wide, twice the detector strip size, to ensure the proper sky image reconstruction. For a detailed description of the experiment we refer the reader to Soffitta et al. (2006) and to references therein. Instrument calibrations have been done with imaging radioactive sources at finite distances as well as with an X-ray tube (Evangelista et al. 2006). Among the main goals of such calibrations are to sample the instrumental point spread function at some crucial off-axis angles complementing and cross-checking in-flight calibrations, to estimate the focal distance of each of 4 detectors and finally to improve our understanding about the real mask-detector geometry.

Given the short time available for this first set of on-ground calibrations, we had to limit our measurements to two radioactive sources: a strong ^{109}Cd (with emission line at 22 keV) and a ^{137}Cs with line at 32 keV, most appropriate to the SuperAGILE energy band. To allow these calibrations 4 source holders have been built (see Fig.1). The geometry and material of source holders were studied in order to reduce scattering and self-absorption to minimum. The source holders placement has been done with a laser tracker showed in Fig.1 that is able to return a target position respect to an ortonormal system center in it with an intrinsic accuracy of 60 μm. However given the measurements set-up the final accuracy of positioning the source holders respect to the reference optical cubes on the mask plane is 1 mm. If we consider the systematic uncertainty in positioning sources inside the holders this value is a little bit worse. Both radioactive sources were placed at a distance of 204 cm from the detection plane with a lateral displacement of 0 degrees for ^{137}Cs and of 0, 10, 20, 30

Further author information: immacolata.donnarumma@iasf-roma.inaf.it, +39 06-49934117

degrees for ^{109}Cd (see Table 1). The acquired data of ^{109}Cd have been selected in the energy band 20-30 keV. The lower energy cut-off has been done to minimize the energy threshold dispersion of channels (not equalized and calibrated yet at the time of this calibration), that could lead to a wrong reconstructed image, while the higher energy threshold allowed to limit the background due to the environmental radioactivity and to the 88 keV photons from the same source that are not absorbed by the Tungsten mask and pass through it without being coded. Moreover, an environmental background, measured during 3600 s, was subtracted from source counts after proper normalization. For the measurements with ^{137}Cs we followed a different approach. ^{137}Cs emits photons at 32.19 keV and 661.7 keV. The latter are not coded by the mask and significantly increase the background counts due to the Compton scattering in detector and other SuperAGILE components. To subtract this background from source counts we have performed a 23700 s long additional measurement shielding the ^{137}Cs source with a 1 mm thick copper sheet. This sheet absorbs $\sim$ 99.97% of 32.19 keV while the fraction of photons absorbed and scattered at 661.67 keV is $\sim$ 6%. After subtracting this self-induced background, the resulting counts have been selected in the energy band 25-40 keV.

The technique applied to imaging of sources with coded mask instrument is a little bit different from that used in the infinite case due to the beam divergence.

In the next section we discuss the standard deconvolution procedure, showing a method developed to suppress the defocussing artifacts introduced by the finite distance.

In section 3 we show the reliability of the adopted focussing procedure by means of computer simulations.

In section 4 we will discuss the preliminary results obtained from radioactive sources imaging.

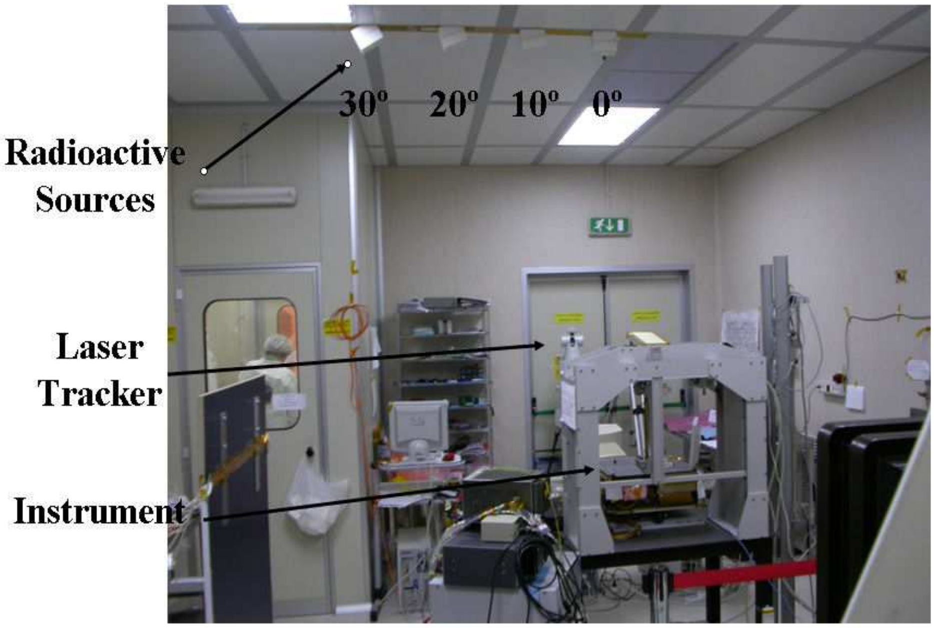

Figure 1. Experimental set-up

2. IMAGING FINITE DISTANCE SOURCES

Imaging sources through the "coded mask aperture imaging technique" means reconstructing the source flux and positions from the aperture shadow on the detector. The size of the shadow depends on the distance to the source, while the location of the shadow depends on the lateral displacement of the source (the angle respect to the zenith). Consider briefly the case of an infinite distance source. The size of the shadow does not vary across the detector because source photons are parallel. Hence we have only a degree of freedom represented by the angular displacement of the source. Recostructing source position and fluxes means to correlate the recorded

	I [μCi]	E [keV]	$\theta_x[deg]$	$\theta_y[deg]$	z [mm]	T [s]
^{137}Cs	95	32.19, 661.67	-0.15 $\pm$ 0.03	0.46 $\pm$ 0.03	1904 $\pm$ 1	42220
^{109}Cd	76	21.99, 88.04	-0.15 $\pm$ 0.03	0.46 $\pm$ 0.03	1897 $\pm$ 1	3600
			9.58 $\pm$ 0.03	0.75 $\pm$ 0.03	1910 $\pm$ 1	6000
			19.62 $\pm$ 0.03	0.62 $\pm$ 0.03	1921 $\pm$ 1	4200
			28.90 $\pm$ 0.03	0.69 $\pm$ 0.03	1920 $\pm$ 1	14400

Table 1. The radioactive sources spectral features, source holders positions (in the SuperAGILE reference frame) and integration time.

image with decoding patterns. If we represent the detector image of the sky with D, then D is given by the convolution of the mask pattern M and the true sky image S:

$$D = S \otimes M. \tag{1}$$

It is possible to reconstruct the sky image S' through a cross-correlation of the detector image with a certain reconstruction matrix R, which has to be defined:

$$S' = D \odot R = S \otimes (M \odot R). \tag{2}$$

It is obvious that the reconstruction will be perfect when $M \odot R$ is the identity matrix. This can be achieved if the mask is based on a pseudo-random URA pattern (see e.g. in 't Zand, 1992). If the complete pattern of such mask is projected on the detector then $S' = S$ (disregarding noise). For mask-detector systems where the mask has the size of detector, as in SuperAGILE, this is true only for the on-axis position. For any other direction in the sky the coding noise due to the partial sampling of the mask pattern emerges (e.g. in 't Zand, 1992).

Focussing finite distance source is more complicated because the size of the shadow in the detector plane is magnified depending on the distance from the source to the plane itself. Using simple geometrical considerations (see Fig.2) the magnification m of the mask pattern size is related to the distance from the source to the mask plane (say z) and to the mask-detector separation f:

$$m = (z + f)/z. \tag{3}$$

Substantially the finite distance source introduces "defocussing artifacts" that need to be removed. The correction, consisting in a collimation of the photons collected on the detector, could be done for istance in the following ways:

- magnifying the mask pattern by a factor m, then applying formula (2) to obtain the correct object distribution;
- shrinking the detector image while keeping the mask pattern fixed and again applying (2) (hereafter the "shrinking procedure").

We have analyzed both options, but to keep the same configuration of mask-detector system (i.e. the same correspondence between mask element and detector pixel) we have developed a reconstruction method based on a virtual detector shrinked by a factor $1/m$. Both procedures provide results in substantial agreement.
In this paper, we will focus on the "shrinking procedure".

2.1. The shrinking procedure

Suppose to have an r-elements vectors for detector, *shrinking* means to redistribuite all the counts, i.e. by linear interpolation, on a new array with dimension n equal to a fraction $z/(z + f)$ of the original size (putting the last $r - n$ elements equal to zero). The perfect suppression of defocussing artifacts needs the accurate knowledge of factor m, that is of both distance from the source to the mask plane and the detector-mask separation. It is possible to overcome the knowledge of these quantities developing a procedure that searches for the brightest peak of source counts over a range of distances from the source to the detector plane (that is varying m).

The best suppression is obtained when the correct magnification factor is found. For the on-axis position this can be achieved searching for the maximum of the brightest peak and for a symmetric point spread function. For off-axis positions the point spread function is no longer symmetric. The two values to be altered during the search for the brightest peak are:

- $z/(z+f)$ (hereafter "the shrinking factor")
- the center of the shrinking in the detector domain (hereafter "the shrinking base point").

The maximum in both variables provides source distance from the mask plane z by means of the correct shrinking factor, known the focal distance (or viceversa); the lateral displacement of the source with respect to the zenith is provided by both z and the shrinking base point. The bidimensional maximum as a function of the z distance presents an absolute maximum, while it is a *periodic* function in the shrinking base point domain. In the latter case the relative maxima are generated when a line drawn from the source position meets the center of the illuminated mask pattern. The shrinking base point corresponding to the maximum is generated by the intersection of this line with the detector plane (see Fig. 2, the short dashed line passing through mask element center represents one of the directions respect to which the shrinking starts). The frequency of the function in the detector domain decreases when source distance increases. When $z \to \infty$ (it means closer to the infinite distance case) the bidimensional maximum as a function of the shrinking base point becomes an almost constant function (as a consequence of collimated photons). In Fig. 3 the 3D plot represents the behaviour of the bidimensional maximum described above for a point-like source placed at 250 cm from the detector plane, showing the periodicity of the bidimensional maximum in the shrinking base point domain (the frequency is about 18 pixel for this distance).

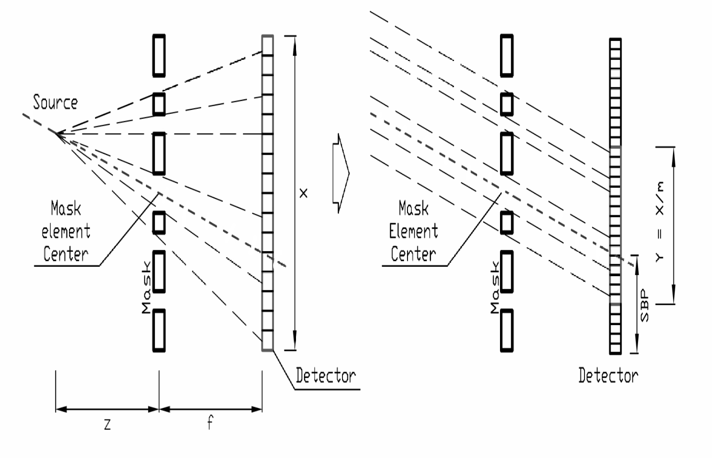

Figure 2. Left: the beam divergence at finite distance is shown; right: a simple scheme that summarizes the "shrinking procedure"; short dashed line indicates one of possible directions with respect to which omnidirectional photons will be collimated.

From geometrical point of view one expects to have a symmetrical point spread function as a result of the shrinking procedure. Little asymmetry may be present due to the computational accuracy and can be neglected. Consequently we consider any asymmetry in the reconstructed point spread function to be associated with real physical and geometrical effects in the instrument.

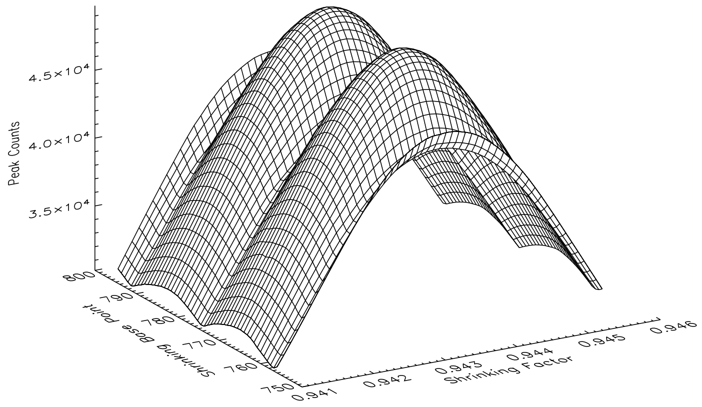

Figure 3. 3D plot of bidimensional maximum function shape of a simulated point-source at z=250 cm from the detector plane.

3. COMPUTER SIMULATIONS OF CLOSE-UP EFFECTS

To check the reliability of this method we have performed Monte Carlo simulations of a large set of sources. We simulated both point-like sources as well as extended sources, varying their positions both in z (source mask-plane distance) and along the plane parallel to the mask to study the accuracy of the focussing method as a function of distance and angular displacement.

The left panel of Fig. 4 shows the image of a simulated point source at $z + f = 250$ cm from the detection plane obtained with the standard deconvolution method (see equation 2.). The right panel of the same figure shows the significant peak emerging after the shrinking procedure has been applied.

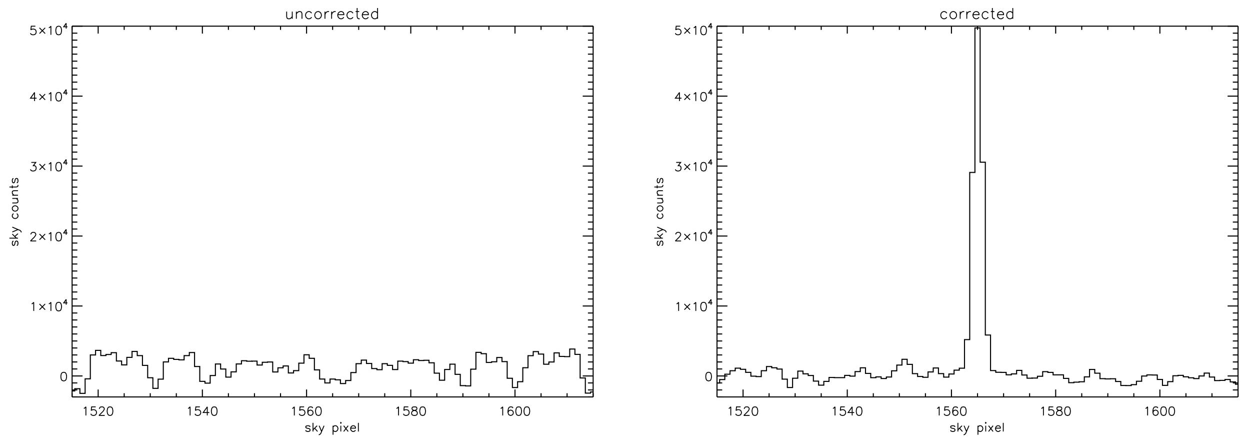

Figure 4. The left panel shows the image of a point source simulated at $z + f = 250$ obtained with the standard deconvolution method; the right panel shows the image obtained for the same source after the application of the shrinking procedure.

Given the mask-detector configuration of SuperAGILE (being the ratio of detector strip to mask element 1:2) we expect that an on-axis source at infinite distance has a 2 or more detector pixels FWHM. It is reasonable to suppose that interpolation leads to some systematic, leading for example to a wider corrected and deconvolved image. It is possible to estimate the widening due to interpolation comparing the deconvolved image of an infinite distance source with that obtained for a source at finite distance, say $z + f = 250$ cm. To this purpose we have simulated an infinite distance source at 2 degrees off-axis (corresponding to the maximum beam divergence) where no widening of point spread function due to the off-axis position is expected. Thus, we can estimate image widening due only to the interpolation procedure. The comparison between the reconstruced images of both simulated sources is shown in Fig. 5. The interpolation leads to a reduction of the peak counts of $\sim$ 20%. This peak-counts attenuation becomes greater if one considers an extended source: for a radioactive source caesium-like (with a $\sim$32 keV line), with a disk shape with a 5 mm diameter we predict a factor of $\sim$ 40%. It is clear that this further widening depends on the spatial profile of the source.

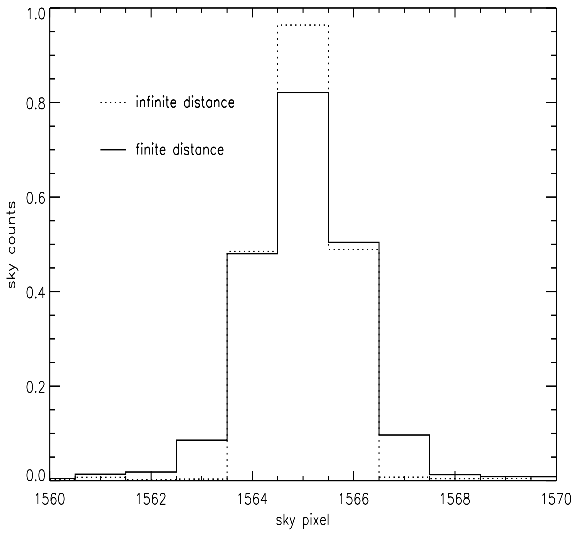

Figure 5. Dot line: reconstructed skyimage of point source at infinite distance (obtained using the stardard deconvolution method; solid line: focussed image of same source simulated at finite distance (say z=250 cm).

The reconstruction procedure also allows to calculate both the z distance and the lateral displacement of the source (hereafter y). By means of Monte Carlo simulations we have calculated the errors in both directions associated with statistical fluctuations. In particular, if we move around the simulated z-position by a step of ± 2.5 cm the resulting error $|\Delta z| \simeq 0.1$ cm. With regard to the angular displacement of the source an accuracy of $|\Delta \mathrm{y}| \simeq 0.0045$ cm is achieved.

Computer simulations have been used for two main aims: validating the performance of the focussing procedure as described above; driving set-up of calibrations with radioactive sources in laboratory. This procedure should allow:

- to estimate the mask-detector separation (focal distance) from the calculated magnification factor and known z (see equation 3);
- to calibrate the relation between the detector pixel and the angular displacement in the sky given the relation $y = z \times arctg(angle) + shrinkingbp \times stripdim + cc$ (where shrinkingbp is the shrinking base point, stripdim is the detector strip length and finally cc is a correction parameter related to the detector geometry) and the $\sim 45\mu$m accuracy of reconstructed y we obtain that the angle is determined with accuracy $< 1/40$ of SuperAGILE pixel going at $z + f > 200$ cm;
- to study instrumental point spread function variation as a function of off-axis position;
- to estimate the effective area at energy associated with imaged sources.

A set of simulations were performed to determine these physical quantities. In particular we scanned different z distances to the detector plane. The choice of distance ranges is related to the results aimed to achieve: tomography is best achieved by imaging source from a distance as short as possible; to understand detector response while imaging infinite distance sources needs to go farther from the detection plane ($z \to \infty$ is equivalent to $m \to 1$). Imaging source very close to the detection plane gives rise to important side effects: "inverse square" and "obliquity effects". The radiation intensity reaching the detector is no longer uniformely distributed because its pathlength r' increases going far from the normal vector r ("inverse square effect"). Moreover, the angular subtense of each hole decreases across the aperture ("obliquity effect") leading to flux attenuation proportional to it. Since tomographycal studies are beyond this paper aims, we refer to Cannon & Fenimore (1979) for details about the inverse square and obliquity effects.

For our purposes we studied different z distances to the detector plane from 100 cm up to 300 cm (for SuperAGILE this means from $m \sim 1.1$ to $m \sim 1.05$) to fix a distance for the calibrations set-up that represented a good trade-off between the accuracy in the reconstruction method and the integration time needed for the available radioactive sources. At these distances the inverse square and obliquity effects are negligible. On the basis of the observed deconvolved images features such as the peak counts, the point spread function widening, shape systematic asymmetry, we found no reason to discriminate among these distances. However for one of our goals, the estimation of the focal distance f it is clear that the farther the point source is better the accuracy of f can be. In particular assuming a $z + f$ distance of $\sim$ 200 cm and taking the accuray in reconstruction of z (and then of m) into account, we predict an accuracy of $\sim$75 μm of f estimation (it is $\sim$ 165 μm at $z + f = 100$ cm). The focal distance is present in the relation that allows to calculate the lateral displacement of source in the sky from detector pixel. Since the error of sky direction reconstruction as a function of f is given by $1/2 \times sin(2\theta) \times \Delta f / f$ a Δf equal to 75 μm corresponds for a 30 degree off-axis positions to accuracy of 0.013 degrees, while $\Delta f = 165$ μm corresponds to 0.028 degrees. Comparing these accuracies with a value of $\sim$ 0.036 degrees for sky pixel at 30 degrees we deduce that distance greater than 200 cm allow to determine the sky direction with a precision that is well below the corresponding pixel size. We underline as the 0.013 degrees accuracy is below the $\sim$ 0.016 degrees accuracy expected for the attitude correction due to satellite motion. Moreover, the 0.0045 μm accuracy in the calculation of y shows again as distance greater than 200 cm from the detection plane will improve the pixel-degree conversion: this accuracy falls below 1/40 of detector pixel (keeping the same statistics at all distances). So we requested a source distance equal or greater than 200 cm for SuperAGILE calibrations. However all the previous accuracy discussions assume that we preserve the statistics at any distance. Hence this suggests to not move too far from the 200 cm, in order to avoid large increase in the integration time needed.

4. LABORATORY RESULTS

Here we show preliminary results of SuperAGILE calibration with radioactive souces at finite distance. In Fig. 6 we show the reconstructed images of ^{109}Cd from 0 to 30 degrees obtained applying the shrinking procedure. Given the $z+f$ distances inferred by the metrological measurements and the magnification factors resulting by the application of our shrinking procedure we estimate the focal axis distances for all of the angular displacements. They lead to a mean value of 142.49 mm (see Fig. 7) with a standard deviation of 0.16 mm. The value calculated at 9.58^o indeed deviates significantly from the nominal focal distance, 142.4 mm. Considering the value of m calculated at 9.58^o and assuming the nominal value for the focal distance, the reconstructed z distance from the mask plane results 4 mm lower than that returned by the laser tracker (we remind that the overall position error due to the laser tracker is 1 mm). Then one possibility is that during the acquisition the source moved inside its holder. If we exclude this measurement in the mean value calculation, we obtain a mean value $\overline{f} = 142.44$ mm and $\sigma = 0.10$ mm. However it has to be taken into account that the variation of distances observed for different angular displacements could indicate a not perfect parallelism between mask and detector planes as well as mask imperfections. In fact, when one goes far from the on-axis position, a more partial projection of the whole mask pattern is present on the detector and then it is easier to observe local deviations from the ideal configuration of the experiment rather than when all the pattern is projected; in the second case the geometrical distorsions of the mask are averaged over the whole detector. However these prelimiary calibrations gave us clues of such geometrical distorsions that have to be corroborated first with the additional on-ground calibrations that will be performed at satellite level and after with in-flight calibrations.

In Table 2 the value of the peak counts and of the total counts of detector are listed. We stress that the fraction of the total counts covered by the peak varies from $\sim 70\%$ for ^{109}Cd to $\sim 60\%$ for ^{137}Cs indicating a different intrinsic spatial profile of these sources. Indeed laboratory measurements of the spatial distribution of the radionuclide within the source are planned. The results of these measurements will allow us to extract from ^{109}Cd and ^{137}Cs images their spatial profiles together with the systematics introduced by the shrinking procedure, i.e. due to the linear interpolation. To this purpose we developed a maximum likelihood procedure to estimate the point spread function, focussing finite distance radiactive sources. Given the focussed images obtained in laboratory, we simulate detector response of a finite distance source placed at the same reconstructed distance as the radioactive source and with the same spatial profile (it requires the convolution of the source spatial profile with mask and a sort of expansion of the detector pixel counts taking into account the finite distance). The second step is to apply the shrinking procedure (deconvolution) so to obtain the simulated source, $SimulSource$. Hence we are able to define the iterative function

$$psf_{n+1} = psf_n + \alpha * (RealSource - SimulSource_n) \tag{4}$$

where $psf_0 = RealSource$ e $SimulSource_0 = SimulSource$ and α is a correction index, for which a typical value is 0.2.
For all next iterations we obtain $SimulSource_n$ by:

- Convolution of source spatial profile with mask
- Expansion of detector pixel counts given the magnification factor inferred by focussing procedure applied to the real source image.
- Convolution of such detector with psf_{n+1}
- Deconvolution of obtained magnified detector image (using the shrinking procedure).

We will reach the convergence and hence the corrected instrumental PSF when $SimulSource_n \longrightarrow RealSource$. A similar approach has been used for on-ground calibrations with X-ray tube. Evangelista et al. 2006 show a preliminar point spread function obtained for SuperAGILE applying the likelihood procedure. It will be compared with one that we will obtain from the source acquisitions at finite distance once their profiles will be known.

	θ_x **[deg]**	m	z **[mm]**	f **[mm]**
^{137}Cs	-0.15 $\pm$ 0.03	1.07481 $\pm$ 0.00003	1904 $\pm$ 1	142.44 $\pm$ 0.075
^{109}Cd	-0.15 $\pm$ 0.03	1.07508 $\pm$ 0.00003	1897 $\pm$ 1	142.43 $\pm$ 0.075
^{109}Cd	9.58 $\pm$ 0.03	1.07473 $\pm$ 0.00003	1910 $\pm$ 1	142.73 $\pm$ 0.075
^{109}Cd	19.62 $\pm$ 0.03	1.07421 $\pm$ 0.00003	1921 $\pm$ 1	142.56 $\pm$ 0.075
^{109}Cd	28.90 $\pm$ 0.03	1.07412 $\pm$ 0.00003	1920 $\pm$ 1	142.31 $\pm$ 0.075

Table 2. The magnification factor m and the resulting focal distances obtained assuming the distances given by the laser tracker for ^{109}Cd and ^{137}Cs.

5. CONCLUSIONS

We have presented the preliminary results achieved during the first phase of SuperAGILE on-ground calibrations based on focussing radioactive sources at finite distance. This has requested to implement a procedure able to clean the deconvolved image by the defocussing artifacts introduced by the beam divergence. We have checked this procedure by means of Monte Carlo simulations of sources imaged at finite distance studying the accuracy of this method. Given the dependence of reconstruction accuracy on the source placements these drove the experiment set-up. We underline the accuracy of $\sim 45\mu$m in the calculation of the lateral displacement and

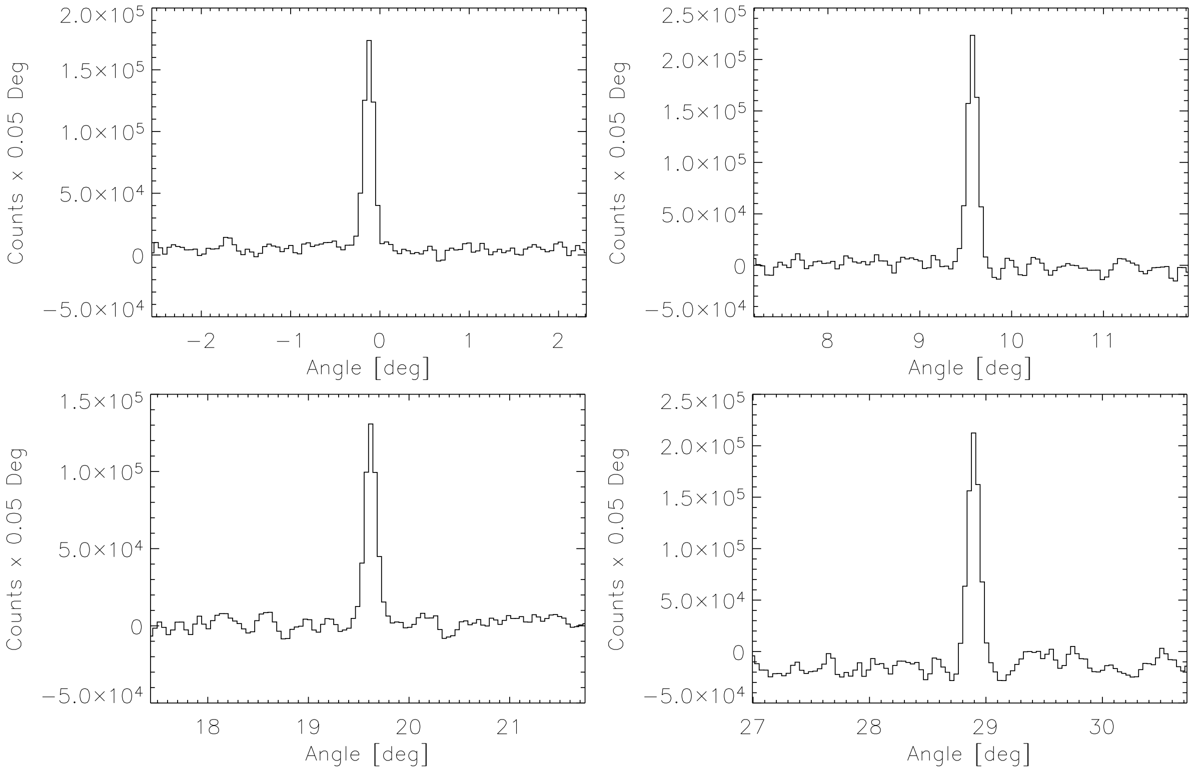

Figure 6. The deconvolved images of ^{109}Cd resulting from the shrinking procedure are shown from 0 to 30 degrees.

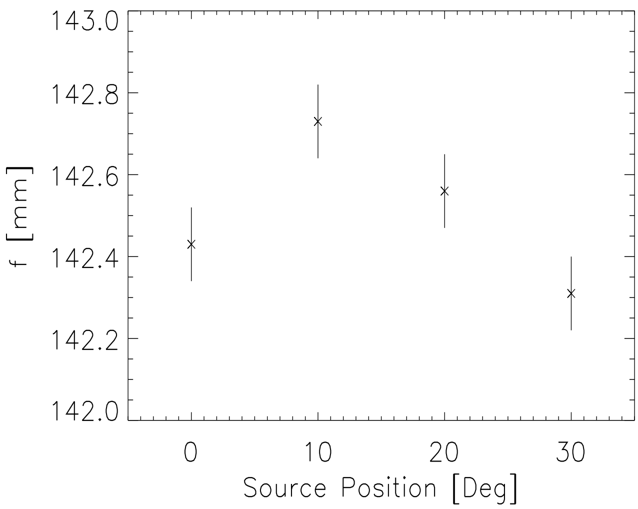

Figure 7. Focal distances reconstructed for ^{109}Cd as a function of its angular positions.

of $\sim$ 1 mm in the reconstruction of source distance to the mask plane that is in good agreement with the metrological reconstruction with laser tracker used during the calibrations. We have imaged ^{109}Cd and ^{137}Cs at $\sim$ 200 cm. The deconvolved images obtained for both sources have given a first estimation of the focal distance to be compared with the nominal value inferred by the experiment geometry and mechanics. This value seems to be confirmed within a standard deviation of $\sim$ 100μm evaluated on different off-axis positions from 0 to 30 degrees. Such error may indicate some deviations of the geometry from the ideal configuration; that is the presence of not perfect parallelism between the mask and detector planes, mask imperfections or nonplanarity.

	θ_x [deg]	**Source counts**	**Peak counts**	**%** ($\mathbf{cnt}_{im}/\mathbf{cnt}_{tot}$)	**S/N**
^{137}Cs	-0.15 ± 0.03	155758	98430	63	167
^{109}Cd	-0.15 ± 0.03	226539	173697	76	429
^{109}Cd	9.58 ± 0.03	295857	223486	76	478
^{109}Cd	19.62 ± 0.03	180546	130156	75	367
^{109}Cd	28.90 ± 0.03	266647	212404	79	386

Table 3. Source positions from laser tracker, total counts, peak counts, fraction of source counts collected in peak and signal to noise ratio of our measurements.

It is clear that further calibrations will be used to better investigate the geometry. This will lead together with the accuracy in the reconstruction of the lateral displacement of the source to calibrate the conversion between detector pixel and sky degrees.

The calibration of the point spread function, at least for some crucial off-axis positions, is possible due to the maximum likelihood procedure developed to remove systematics and source profile from the deconvolved images.

ACKNOWLEDGMENTS

The SuperAGILE Team is grateful to Pietro Ubertini and to all the IBIS Team for making the clean room facility available for SuperAGILE testing and calibrations. We want to thank M. Trifoglio, A. Bulgarelli and F. Gianotti for providing and continuously supporting the DISCoS system for SuperAGILE.

REFERENCES

1. T. M. Cannon and E. E. Fenimore, 1979, Applied Optics, vol. 18, 1052.
2. Y. Evangelista et al., these proceedings.
3. in't Zand, J.J.M., 1992, PhD Thesis.
4. P. Soffitta et al., these proceedings.